


 Cite this: *CrystEngComm*, 2015, 17, 8130

Selective gelation of *N*-(4-pyridyl)nicotinamide by copper(II) salts†

 Dipankar Ghosh,^a Ieva Lebedytė,^a Dmitry S. Yufit,^b Krishna K. Damodaran^{*a} and Jonathan W. Steed^{*b}

We report the selective gelation properties of the copper(II) complexes of *N*-(4-pyridyl)nicotinamide (4PNA). The morphology of the xerogels was examined by scanning electron microscopy (SEM). The correlation between the X-ray powder diffraction (XRPD) pattern of the xerogels and the single crystal structure of the copper(II) acetate complex suggests that the single crystal X-ray data represent a good structural model for the gel fibers, and that gelation arises from the presence of a 1D hydrogen-bonded chain between gelator amide groups and coordinated anions, while the presence of strongly bound water in non-gelator systems results in the formation of more extensively hydrogen-bonded crystalline networks. The selective gelation of all the copper(II) salts compared to the other metal salts may be attributed to the Jahn–Teller distorted nature of copper(II), which weakens water binding in all copper(II) salts.

 Received 7th May 2015,
Accepted 18th August 2015

DOI: 10.1039/c5ce00901d

www.rsc.org/crystengcomm

Introduction

Supramolecular gels based on low molecular weight gelators (LMWGs)^{1–10} have emerged as a prolific area of current research due to their potential applications as functional soft materials for separation,¹¹ drug delivery,^{12–14} as well as templating of inorganic and polymer materials^{15,16} and as media to control crystal growth.¹⁷ Gels are formed by the immobilisation of solvent molecules in the 3D fibrous network of the gelators, which self-assemble *via* non-covalent interactions^{18,19} such as hydrogen bonding, van der Waals interactions, π – π stacking and halogen bonding. Recently, there has been an upsurge of interest in metal-based supramolecular gels (metallogels).^{8,20} These metal-containing LMWGs have strong coordination interactions between the organic moiety and metal centre, which act as a key driving force in the formation of the gel fibre network in combination with various non-covalent interactions.^{8,21,22} The gel fibres themselves can arise from the self-assembly of discrete complexes,^{23–28} coordination polymers,^{29–34} or cross-linked

coordination polymers.³⁵ Non-coordinated metal ions or metallic nanoparticles may also be incorporated into the gel matrix.^{36–39} The inclusion of metal ions in LMWGs leads to the formation of multifunctional metallogels which offer potential applications²⁰ in catalysis, sensing, optics and magnetic materials.

The understanding of the structure of LMWGs and metallogels in the gel state is still in its infancy because of the low ordering of the gel as a whole and the wide range of length scales of the gel structure from the nano- to the micro-scale. Efforts have been made to determine the gel structure by analysis of the X-ray diffraction pattern of the dried gel (xerogel). Nevertheless, removal of solvent to prepare a xerogel can result in artefacts due to dissolution and recrystallization, changes in morphology or polymorphic phase transition. However, the combination of the crystal structure and the powder diffraction pattern of either a native gel or a xerogel remains one of the most practical methods to gain insight into the gelator structure and aggregation behaviour. Based on this approach, efforts have been made to identify the key structural features of gel network formation in LMWGs by analysis of their potential using supramolecular synthons.⁴⁰

Although there are a few reports on the structure–property correlation of metallogels,^{41–45} designing metallogels with specified properties and structures is still a daunting task. We have shown that binding of metal to functional groups such as a pyridyl group can ‘switch on’ gelation by removing the competing urea–pyridyl hydrogen bonding interaction.^{18,46} In previous work, one of us has reported a series of pyridyl amide compounds and

^a Department of Chemistry, Science Institute, University of Iceland, Dunhagi 3, 107 Reykjavík, Iceland. E-mail: krishna@hi.is; Fax: +354 552 8911; Tel: +354 525 4846

^b Department of Chemistry, Durham University, South Road, Durham DH1 3LE, UK

† Electronic supplementary information (ESI) available: Crystallographic information in CIF format for the structure of 1, 2, 3 & 4. Details of gelation experiments, PXRD comparison, SEM of copper(II) nitrate gel and T_{gel} measurement. CCDC 1062590–1062592 and 1062883. For ESI and crystallographic data in CIF or other electronic format see DOI: 10.1039/c5ce00901d



established that *N*-(4-pyridyl)isonicotinamide can selectively form a hydrogel.⁴⁷ Other *N*-(pyridyl)isonicotinamide isomers do not form hydrogels, highlighting the importance of the relative position of ring nitrogen atoms for gel formation. In this work, we explore the ability of metal salts to bring about gelation in pyridyl amides. Specifically, we report the gelation properties of the metal salts of *N*-(4-pyridyl)nicotinamide (4PNA) as depicted in Scheme 1.

Experimental

Materials and methods

All starting materials were purchased from commercial sources and were used as supplied. Dichloromethane was freshly distilled from calcium hydride prior to use for the synthesis of amide, while the other solvents were used without further purification. Deionized water was used for all the experiments. ¹H and ¹³C NMR spectra were recorded on a Bruker Advance 400 spectrometer (¹H-NMR: 400 MHz, ¹³C-NMR: 100 MHz). IR spectra were measured on a Nicolet iS10, SEM was performed on a Leo Supra 25 microscope and PXRD was carried out using a Bruker D8 Focus instrument.

Synthesis of the ligand

The synthesis and characterisation of 4PNA have been reported previously⁴⁷ and the analytical and spectroscopic data matched those reported in the literature.

Synthesis of complexes

[Cu(4PNA)₂(OAc)₂] (1). A solution of 4PNA (25 mg, 0.125 mmol) in 5 mL of ethanol was layered over 5 mL of aqueous Cu(OAc)₂·2H₂O (12.4 mg, 0.062 mmol) solution. Blue crystals of 1 were obtained in a week (23 mg, 0.04 mmol). Yield: 64%. Anal. data for C₂₆H₂₄CuN₆O₆: calc. C, 53.84; H, 4.17; N, 14.49. Found: C, 53.72; H, 4.04; N, 14.42. FT-IR (cm⁻¹): 3255m, 3171m, 3075m, 3002m, 1687vs, 1601vs, 1507vs, 1429vs, 1332s, 1298s, 1240w, 1209w, 1117s, 1065w, 1026s, 895m, 839s, 728s, 679m, 622m, 601m, 542s.

[Cd(4PNA)₂(OAc)₂(H₂O)]·2H₂O (2). The cadmium complex was synthesised by layering an ethanolic solution (1.5 mL) of 4PNA (20 mg, 0.1 mmol) over an aqueous solution (1 mL) of Cd(OAc)₂·2H₂O (13.3 mg, 0.05 mmol). Colourless crystals suitable for X-ray analysis were obtained after a period of one week (8 mg, 0.012 mmol). Yield: 25%. Anal. data for C₂₆H₃₀CdN₆O₉: calc. C, 45.72; H, 4.43; N, 12.31. Found: C,

45.87; H, 4.12; N, 12.30. FT-IR (cm⁻¹): 3247w, 3170w, 3069w, 1686s, 1597vs, 1523vs, 1421vs, 1333s, 1301s, 1212s, 1117s, 1065w, 1045m, 1015s, 936w, 896m, 834s, 730s, 711s, 672m, 622m, 591m, 538s.

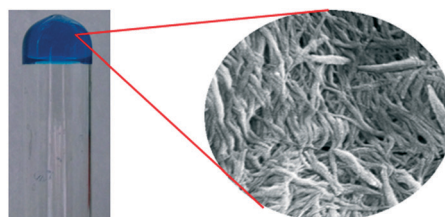
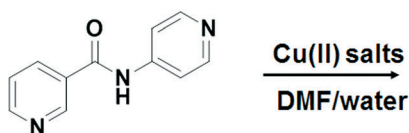
[Zn(4PNA)₂(NO₃)₂(H₂O)₂] (3). Complex 3 was synthesized by layering an ethanolic solution (10 mL) of 4PNA (39.8 mg, 0.2 mmol) over an aqueous solution (10 mL) of Zn(NO₃)₂·6H₂O (29.7 mg, 0.1 mmol). After a period of two weeks, X-ray quality single crystals were obtained (48.6 mg, 0.078 mmol). Yield: 78%. Anal. data for C₂₂H₂₂N₈O₁₀Zn: calc. C, 42.36; H, 3.55; N, 17.96. Found: C, 42.27; H, 3.38; N, 17.79. FT-IR (cm⁻¹): 3430b, 2516w, 2427w, 2356m, 1858w, 1678vs, 1620s, 1568s, 1492vs, 1426m, 1384vs, 1341m, 1315m, 1292s, 1108m, 1063s, 1023s, 920m, 900s, 873w, 842w, 828m, 811m, 756m, 700vs, 651s, 602m, 528m, 420m.

[Cd(4PNA)₂(NO₃)₂(H₂O)₂] (4). An ethanolic solution (10 mL) of 4PNA (39.8 mg, 0.200 mmol) was layered over an aqueous solution of Cd(NO₃)₂·4H₂O (30.8 mg, 0.1 mmol). After a period of one week, X-ray quality single crystals were obtained (36.0 mg, 0.053 mmol). Yield: 54%. Anal. data for C₂₂H₂₂CdN₈O₁₀: calc. C, 39.39; H, 3.31; N, 16.70. Found: C, 39.22; H, 3.26; N, 16.64. FT-IR (cm⁻¹): 3668w, 3391b, 3306b, 2446w, 2361s, 1929b, 1769w, 1681vs, 1596vs, 1523vs, 1418m, 1384vs, 1333vs, 1297vs, 1208s, 1115s, 1065m, 1047m, 1021vs, 930m, 897s, 822vs, 729m, 699vs, 596m, 530s, 418m.

Gel preparation

Copper(II) acetate gel. Gels were prepared at various wt% by dissolving the required amount of Cu(OAc)₂·2H₂O in water (0.5 mL) and mixing it with the corresponding amount (1:2 metal:ligand ratio) of 4PNA in DMF (0.5 mL). The mixture was sonicated for 2–4 minutes and allowed to stand overnight. The blue copper(II) acetate–4PNA gel was obtained and confirmed by the tube inversion test. Yield: 45%. The spectroscopic data for the xerogels matched those for 1.

Copper(II) chloride gel. The gelation experiments were performed by mixing an aqueous solution of CuCl₂ (0.5 mL of water) with the corresponding amount (1:2 metal:ligand ratio) of 4PNA in DMF (0.5 mL). The resulting solution was sonicated for one minute and allowed to stand overnight to yield a green gel. Yield: 38%. Anal. data for C₁₇H₂₃Cl₂CuN₅O₃: calc. C, 42.55; H, 4.83; Cu, 13.24; N, 14.60. Found: C, 42.72; H, 4.49; Cu, 13.49; N, 13.84. FT-IR (cm⁻¹): 3303m, 3228m, 3152m, 3066m, 1693vs, 1600vs, 1512vs, 1428s, 1331s, 1297vs,



Scheme 1 Gels obtained by reacting 4PNA and copper(II) salts.



1209s, 1117s, 1049m, 1024m, 896m, 835s, 725w, 696m, 675w, 645w, 599w, 537m, 445w.

Copper(II) nitrate gel. Gelation was observed at 3–7 wt% and the gel was prepared by mixing $\text{Cu}(\text{NO}_3)_2 \cdot 3\text{H}_2\text{O}$ (in water, 0.5 mL) with the corresponding amount (1:2 metal:ligand ratio) of 4PNA in DMF (0.5 mL). The solution was mixed together without sonication and allowed to stand overnight to yield a greenish-blue gel. Yield: 19%. Anal. data for $\text{C}_{14}\text{H}_{18}\text{CuN}_6\text{O}_9$: calc. C, 35.19; H, 3.80; Cu, 13.30; N, 17.59. Found: C, 35.51; H, 3.49; Cu, 12.59; N, 16.10. FT-IR (cm^{-1}): 3319m, 3084w, 1695s, 1600vs, 1513vs, 1429s, 1380vs, 1335s, 1295s, 1211s, 1117m, 1057w, 1029w, 897w, 832s, 738w, 690m, 653w, 599w, 536m, 450w.

Copper(II) perchlorate gel. The gelation experiments performed at various concentrations of $\text{Cu}(\text{ClO}_4)_2 \cdot 6\text{H}_2\text{O}$ and 4PNA in 1:2 DMF/water (v/v) resulted in partial gelation. Gelation was observed above 4 wt% at higher DMF concentration (9:1 DMF/water, v/v) and in pure DMF. This was achieved by mixing a solution of $\text{Cu}(\text{ClO}_4)_2 \cdot 6\text{H}_2\text{O}$ (0.1 mL of water or DMF) with the corresponding amount (1:2 metal:ligand ratio) of 4PNA in DMF (0.9 mL). The resulting solution was sonicated for one minute and allowed to stand overnight to yield a greenish-blue gel. Yield: 13%. Anal. data for $\text{C}_{25}\text{H}_{25}\text{Cl}_2\text{CuN}_7\text{O}_{11}$: calc. C, 40.91; H, 3.43; Cu, 8.66; N, 13.36. Found: C, 41.86; H, 3.11; Cu, 9.69; N, 12.96. FT-IR (cm^{-1}): 3448b, 3069m, 1692s, 1600vs, 1514vs, 1476w, 1425s, 1395w, 1335s, 1298s, 1210s, 1116vs, 1029m, 898w, 834s, 734w, 687m, 627m, 599m, 535m.

Copper(II) sulphate gel. The copper(II) sulphate complexes of 4PNA displayed similar properties as the copper(II) perchlorate salts. In this case, the required amount of $\text{Cu}(\text{SO}_4) \cdot 5\text{H}_2\text{O}$ in water (0.2 mL) was mixed with the corresponding amount (1:2 metal:ligand ratio) of 4PNA in DMF (0.8 mL). The mixture was sonicated for one minute and allowed to stand overnight to yield a greenish-blue gel. Yield: 44%. Anal. data for $\text{C}_{22}\text{H}_{28}\text{CuN}_6\text{O}_{11}\text{S}$: calc. C, 40.77; H, 4.35; Cu, 9.80; N, 12.97; S, 4.95. Found: C, 40.88; H, 3.94; Cu, 10.58; N, 12.96; S, 5.91. FT-IR (cm^{-1}): 3401b, 3084w, 1691s, 1654m, 1605vs, 1516vs, 1421s, 1387w, 1336s, 1302s, 1212s, 1120vs, 1029m, 899w, 839m, 738m, 698m, 652w, 619m, 541m.

Scanning electron microscopy

The copper(II) salt dissolved in water was mixed with a solution of 4PNA in DMF in a 1:2 metal:ligand ratio. In the case of copper(II) acetate, copper(II) chloride and copper(II) nitrate, 1:1 DMF/water (v/v) was used. For copper(II) perchlorate and copper(II) sulphate, 9:1 DMF/water (v/v) and 8:2 DMF/water (v/v) mixtures were used, respectively. It was then allowed to stand overnight. The resulting blue gel was filtered and dried under high vacuum. The copper(II) acetate and copper(II) chloride gels in pure water were also prepared in a similar fashion and dried. A small portion of the dried gel was placed on a pin mount with graphite planchets on top and coated with gold in the SEM (Leo Supra 25 microscope).

Crystallography

X-ray quality single crystals were obtained by slow evaporation of 4PNA and a metal salt solution such as $\text{Cu}(\text{OAc})_2 \cdot 2\text{H}_2\text{O}$ (1), $\text{Cd}(\text{OAc})_2 \cdot 2\text{H}_2\text{O}$ (2), $\text{Zn}(\text{NO}_3)_2 \cdot 6\text{H}_2\text{O}$ (3), $\text{Cd}(\text{NO}_3)_2 \cdot 4\text{H}_2\text{O}$ (4) and $\text{Cu}(\text{NO}_3)_2 \cdot 3\text{H}_2\text{O}$ (5); however, the crystals of 5 did not diffract. X-ray single crystal data have been collected using $\text{MoK}\alpha$ radiation ($\lambda = 0.71073 \text{ \AA}$) on Bruker D8 Venture (Photon 100 CMOS detector, $1\mu\text{S}$ microsource, focusing mirrors for complexes 2, 3 and 4 and for complex 1, sealed tube and graphite monochromator) diffractometers equipped with Cryostream (Oxford Cryosystems) open-flow nitrogen cryostats at a temperature of 120.0(2) K. All structures were solved by direct methods and refined by full-matrix least-squares on F^2 for all data using Olex2 (ref. 48) and SHELXTL (ref. 49) software. All non-disordered non-hydrogen atoms were refined anisotropically, hydrogen atoms in structure 1 were refined isotropically, and the hydrogen atoms in structures 2, 3 & 4 (except those of amide groups and H_2O molecules) were placed in their calculated positions and refined in riding mode. Disordered atoms in structures 3 and 4 were refined isotropically with fixed $\text{SOF} = 0.5$. The crystal data and parameters of refinement are listed in Table S14, ESI†. Crystallographic data for the structures have been deposited with the Cambridge Crystallographic Data Centre as supplementary publication (CCDC 1062590–1062592 and 1062883).

Results and discussion

Synthesis

The 4PNA ligand was prepared by reacting nicotinoyl chloride and 4-aminopyridine in dichloromethane in the presence of triethylamine.⁴⁷ The gelation ability of the free ligand was examined in various solvents (Table S2, ESI†) and gelation was observed only in water at a higher concentration (3 wt%). The gelation ability of 4PNA was further analysed in the presence of various salts of metal ions such as $\text{Mn}(\text{II})$, $\text{Fe}(\text{II})$, $\text{Co}(\text{II})$, $\text{Ni}(\text{II})$, $\text{Cu}(\text{II})$, $\text{Zn}(\text{II})$ and $\text{Cd}(\text{II})$ (Table 1). We have selected various anions of these metal salts with different hydrogen bonding properties such as acetate, chloride, nitrate, perchlorate and sulphate. The copper(II) acetate, cadmium(II) acetate, zinc(II) nitrate and cadmium(II) nitrate complexes of 4PNA were also isolated and structurally characterised by single crystal X-ray diffraction (*vide infra* and ESI†).

Gelation studies

All of the metal salts were screened for gel formation with 4PNA in a variety of solvents; however, the starting metal complexes only proved to be soluble in highly polar solvents, particularly water, DMF and DMSO. Gelation tests were performed *in situ* by mixing the metal salt and the ligand. In a typical experiment, an aqueous solution of the metal salt was mixed with a DMF solution of 4PNA (1:1 or 1:2 metal:ligand ratio), sonicated for a short period of time and left to stand overnight. The manganese(II), iron(II), cobalt(II), nickel(II), cadmium(II) and zinc(II) complexes of 4PNA did not



Table 1 Gelation studies with different metal salts in 1:1 DMF/water (v/v)

Metal salts	Initial observation	Final observation	wt%
Cu(OAc) ₂ ·2H ₂ O	Blue solution (C)	Blue gel (T)	2.0–6.0
Cu(OAc) ₂ ·2H ₂ O	Blue solution (C)	Blue gel (O)	7.0–10.0
CuCl ₂	Light green solution (O)	Green gel (O)	2.6–10.0
Cu(NO ₃) ₂ ·3H ₂ O	Blue solution (O)	Blue gel (O)	3.0–6.0
Cu(ClO ₄) ₂ ·6H ₂ O ^a	Greenish-blue solution (O)	Greenish-blue gel (O)	4.0–11.7
CuSO ₄ ·5H ₂ O ^b	Blue solution	Blue gel (O)	3.5–9.0
Zn(NO ₃) ₂ ·6H ₂ O	Clear solution	Clear solution	3.0–9.0
Zn(OAc) ₂ ·2H ₂ O	Clear solution	Clear solution	3.0–8.0
ZnCl ₂	Clear solution	Crystalline material	3.0–6.0
ZnSO ₄ ·7H ₂ O	Clear solution	White precipitate	3.0–6.8
Zn(BF ₄) ₂ ·H ₂ O	Clear solution	Clear solution	3.0–6.0
Cd(NO ₃) ₂ ·4H ₂ O	Clear solution	White precipitate	3.0–9.0
Cd(OAc) ₂ ·2H ₂ O	White solution	White precipitate	3.0–8.0
CdCl ₂	White solution	White precipitate	3.0–6.0
CdSO ₄ ·8/3H ₂ O	White solution	White precipitate	3.0–6.0
FeSO ₄ ·7H ₂ O	Green solution (C)	Yellow precipitate	3.0–6.0
FeCl ₂ ·4H ₂ O	Yellow solution (C)	Crystalline material	3.0–6.0
Ni(OAc) ₂ ·4H ₂ O	Green solution (C)	Green solution (C)	3.0–6.0
NiCl ₂ ·6H ₂ O	Green solution (C)	Green solution (C)	3.0–6.0
Ni(NO ₃) ₂ ·6H ₂ O	Green solution (C)	Green solution (C)	3.0–6.0
Co(OAc) ₂ ·4H ₂ O	Red solution (C)	Red solution (C)	3.0–6.0
CoCl ₂ ·6H ₂ O	Red solution (C)	Pink precipitate	3.0–6.0
Co(NO ₃) ₂ ·6H ₂ O	Red solution (C)	Red solution (C)	3.0–6.0
MnCl ₂ ·4H ₂ O	Clear solution	Clear solution	3.0–6.0
MnSO ₄ ·H ₂ O	Clear solution	Crystalline material	3.0–6.0
Mn(NO ₃) ₂ ·4H ₂ O	Clear solution	Clear solution	3.0–6.0

C = clear, O = opaque & T = transparent. ^a Gelation experiments were performed in 9:1 DMF/water (v/v). ^b Gelation experiments were performed in 8:2 DMF/water (v/v).

form gels; a clear solution was observed initially and further evaporation yielded precipitates/crystals (Table 1). In contrast, all copper(II) salts formed gels with 4PNA at a 1:2 metal:ligand ratio (assessed by a simple inversion test) in different DMF/water concentrations (Fig. 1).

Addition of varying ratios of copper(II) salts and 4PNA in a 1:1 DMF/water mixture (v/v) established that a ratio of 1:2 metal:ligand resulted in optimal gel formation.

In the case of copper(II) acetate, mixing an aqueous solution of the metal salt and a DMF solution of the ligand (1:2 metal:ligand ratio) resulted in a clear solution from 2 wt% to 6 wt% which formed transparent blue gels after leaving to stand overnight. These gels subsequently yielded crystals over

24–48 h depending on the concentration (2–6 wt%), whereas a higher concentration (above 7 wt%) resulted in the formation of an opaque gel (Fig. 2). However, in a 1:1 metal:ligand ratio, gelation was observed above 4 wt%. We repeated these gelation experiments using copper(II) chloride in a 1:1 DMF/water mixture (v/v) and similar results were obtained. An opaque green solution was obtained by mixing an aqueous solution of the metal salt and a DMF solution of the ligand (1:2 metal:ligand ratio), which formed opaque green gels after leaving to stand overnight at various concentrations (from 2.6 wt% to 10 wt%). Gels were also observed in a 1:1 metal:ligand ratio at 3.3 wt%. The copper(II) nitrate complex of 4PNA formed a gel in a 1:2 metal:ligand ratio at 3 wt%

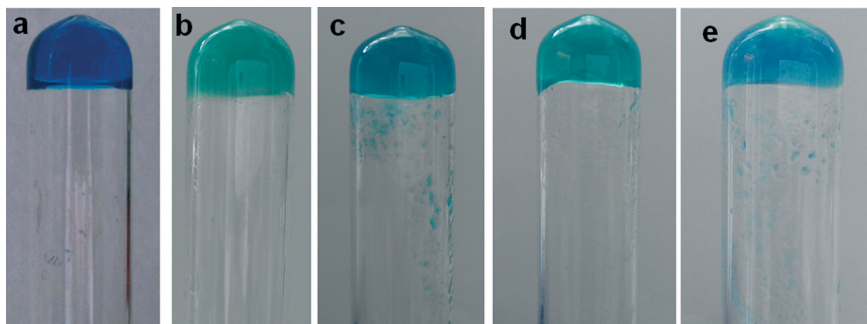


Fig. 1 Reaction of copper(II) salts with 4PNA in a 1:2 metal:ligand ratio forming gels: (a) Cu(II) acetate and 4PNA at 3 wt% in 1:1 DMF/water (v/v); (b) Cu(II) chloride and 4PNA at 3 wt% in 1:1 DMF/water (v/v); (c) Cu(II) nitrate and 4PNA at 4 wt% in 1:1 DMF/water (v/v); (d) Cu(II) perchlorate and 4PNA at 4 wt% in 9:1 DMF/water (v/v); (e) Cu(II) sulphate and 4PNA at 4.5 wt% in 8:2 DMF/water (v/v).



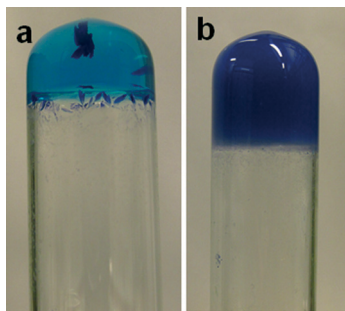


Fig. 2 Reaction of copper(II) acetate with 4PNA (1:2 ratio): (a) crystals and gel formed at 3 wt% of the gelator and (b) opaque gel formed at higher gelator concentration (9 wt%) in 1:1 DMF/water (v/v).

concentration. Gelation was also observed by changing the anion to stronger hydrogen bonding anions, namely perchlorate and sulphate. In the case of perchlorate, gels were observed at a higher concentration of DMF (9:1 DMF/water mixture, v/v) at 4 wt% gelator concentration, whereas for the sulphate anion, gelation occurred at 3.5 wt% in a 8:2 DMF/water mixture (v/v). Increasing the proportion of DMF led to increased solubility and no gelation was observed for copper(II) acetate and copper(II) nitrate. In the case of copper(II) perchlorate, copper(II) chloride and copper(II) sulphate, gelation was observed at higher DMF concentrations.

Similar results were observed in the DMSO/water mixture for all copper(II) complexes. These results indicate that copper(II) coordination selectively enhances the gelation ability of 4PNA, particularly in the case of copper(II) acetate and copper(II) chloride, to a much lesser degree in the other analogues. The selective effect of copper(II) is also noteworthy. The selectivity of metal salts in the gelation process has been reported. The perchlorate and nitrate salts of Ag(I) selectively formed metallogels indicating the importance of metal salts in gelation.⁵⁰ The selectivity of copper(II) chloride salts over other copper(II) salts in metallogel formation has been reported.⁵¹ Recently, the selectivity of copper(II) chloride and bromide over perchlorate, nitrate, sulphate and acetate anions was reported.⁵² These studies reveal the importance of metal salts, specifically copper(II) salts, in metallogel formation. In the present study, a series of copper(II) salts enhanced the gelation properties of the ligand (4PNA) over other metal salts. This is presumably due to the versatile properties of the copper(II) geometry such as its Jahn–Teller distorted nature, which weakens water binding in all copper(II) salts.

Gelation experiments for the complexes of all copper(II) salts were also performed in pure water. Addition of copper(II) acetate and copper(II) chloride to 4PNA (1:2 metal:ligand ratio) in pure water gave gels above 1.5 wt% and 3 wt%, respectively, whereas reaction of other copper(II) salts with 4PNA in water immediately gave a precipitate in every case. These results indicate that DMF acts as a solubilising medium while water acts as an antisolvent. This delicate balance between hydrophobic effects and other intermolecular interactions is required to achieve three-dimensional elastic

self-assembled networks of the gel. These results clearly indicate that the 1:2 metal:ligand ratio is optimal.

Gel thermal stability

The formation of supramolecular gels at room temperature is relatively unusual, implying slow coordination or slow nucleation of the gel fibres. Slow cooling is a more common method to bring about the necessary supersaturated solution from which gel fibre growth can occur. The thermal stability of the room-temperature copper(II) metallogels of 4PNA was evaluated by analysing the temperature at which the gel was converted into a liquid phase (T_{gel}). Copper(II) acetate gels displayed T_{gel} values of 58 °C and 61 °C for 2 wt% and 4 wt%, respectively. The T_{gel} for copper(II) chloride at 3 wt% was 64 °C and that for copper(II) nitrate gels at 6.4 wt% was 53 °C. In comparison, the T_{gel} values for the analogous copper(II) perchlorate and sulphate gels at 4 wt% and 5 wt% were 55 °C and 65 °C, respectively. These results indicate that the thermal stability depends on the hydrogen bonding ability of the anions. The copper(II) acetate and copper(II) chloride gels are thermoreversible at minimum gel concentrations, whereas copper(II) nitrate and copper(II) sulphate gels are thermoreversible at higher concentrations (5–6 wt%). However, prolonged heating at an elevated temperature (<90 °C) resulted in the decomposition of these complexes.

Scanning electron microscopy

The morphologies of the copper(II) gels of 4PNA were studied by SEM analysis. The gels prepared from water and DMF/water (1:1, v/v) were filtered and dried under high vacuum. A small portion of the dried gel was placed on a pin mount with graphite planchets on top and was coated with gold. The SEM images of the copper(II) acetate complex of 4PNA (4 wt%) revealed that both xerogels display a fibrous network, although some crystalline material is also evident in the xerogels obtained from DMF/water (Fig. 3a). This may arise from the drying process given the relative volatility of water compared to DMF, which may well result in partial dissolution and reprecipitation. The width of the gel fibrils varies from 13 nm to 40 nm regardless of the anion and solvent in which the gel is prepared (Fig. S3, ESI†).

Crystal structures

The complexes obtained from the reaction of 4PNA with metal salts such as copper(II) acetate, cadmium(II) acetate, zinc(II) nitrate and cadmium nitrate were characterised by single crystal X-ray crystallography. Crystals were isolated by slow evaporation of an EtOH/water mixture of 4PNA and metal salts. Crystallographic details (Table S14†) and hydrogen bonding parameters (Table S15†) are given in the ESI.†

Crystalline structure of [Cu(4PNA)₂(OAc)₂]. X-ray quality crystals were obtained by slow evaporation of an ethanol–water mixture of copper(II) acetate and 4PNA to give a mononuclear 1:2 complex of formula [Cu(4PNA)₂(OAc)₂] (1), with a



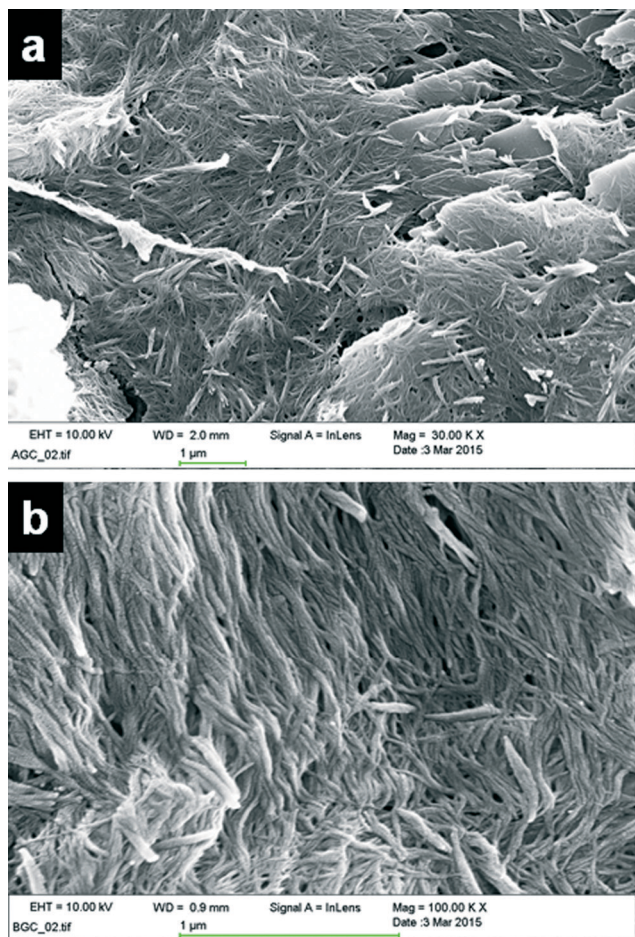


Fig. 3 SEM images of 1:2 copper acetate gels of 4PNA (a) in DMF/water and (b) in only water, displaying a fibrous network.

stoichiometry consistent with the optimal ratio required for gel formation.

The copper(II) metal centre lies on an inversion centre and displays a Jahn–Teller distorted octahedral geometry with the oxygen atoms of the acetate anion adopting an asymmetric chelate coordination mode in the equatorial position. The axial positions are occupied by the pyridyl nitrogen atoms of the 4PNA ligands which coordinate *via* the 4-aminopyridine-derived end of the molecule. The nicotinoyl-derived pyridyl group is uncoordinated in the structure and does not take part in strong intermolecular interactions. The nitrogen atom of the amide moiety of 4PNA is hydrogen-bonded to the oxygen atom of the metal-coordinated acetate anion resulting in the formation of a 1D hydrogen-bonded chain (N \cdots O = 2.8188(19) Å, \angle N–H \cdots O = 164.0(17) $^\circ$). This type of structure could give rise to hydrogen-bonded 1D fibre formation and hence gelation⁵³ (Fig. 4b).

Crystalline structure of [Cd(4PNA)₂(OAc)₂(H₂O)]·2H₂O. Slow evaporation of a solution of cadmium(II) acetate and 4PNA in EtOH/water at a 1:2 metal:ligand ratio resulted in the formation of a complex of formula [Cd(4PNA)₂(OAc)₂(H₂O)]·2H₂O (2) over a period of one week. Although the coordination modes of acetate and 4PNA are similar to those in 1, water coordination results in a distorted pentagonal bipyramidal Cd(II) metal centre (Fig. 5a). The nitrogen atom of the amide moiety of 4PNA displays hydrogen bonding to the metal-coordinated acetate anion resulting in N–H \cdots O interactions (N \cdots O = 2.856(2)–2.950(2) Å, \angle N–H \cdots O = 166(3)–172(2) $^\circ$). The uncoordinated water molecules are hydrogen-bonded to the oxygen atoms of the metal-bound acetate anions. One of these water molecules is further hydrogen-bonded to the nitrogen atom of the nicotinoyl-derived pyridyl

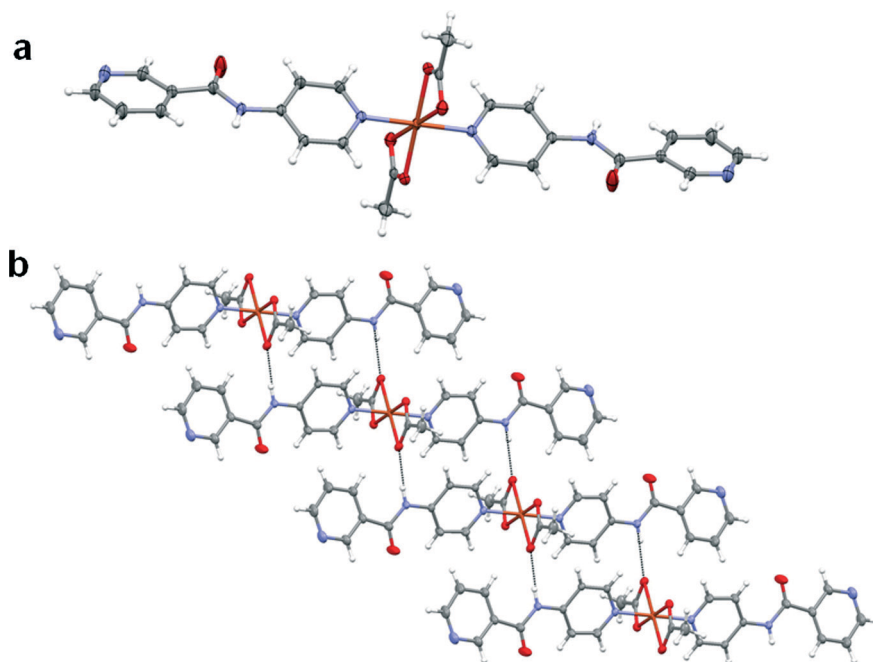


Fig. 4 (a) Molecular structure of 1 and (b) the 1D hydrogen-bonded chain observed in the solid state.



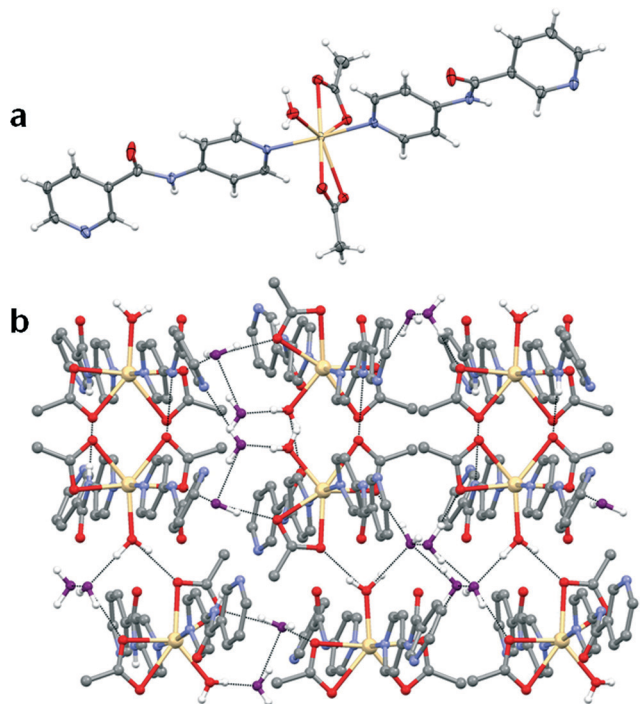


Fig. 5 (a) Molecular structure of **2** (uncoordinated water molecules are not shown) and (b) the 2D hydrogen-bonded chain observed in the solid state (uncoordinated water molecules are shown in purple).

group resulting in the formation of a 2D hydrogen-bonded network (Fig. 5b). The cross-linking provided by the hydrogen bonding to the additional water molecules may explain why this material forms a crystalline solid rather than a gel.

Crystalline structure of $[\text{Zn}(\text{4PNA})_2(\text{NO}_3)_2(\text{H}_2\text{O})_2]$. Single crystals of formula $[\text{Zn}(\text{4PNA})_2(\text{NO}_3)_2(\text{H}_2\text{O})_2]$ (**3**) suitable for X-ray analysis were obtained by slow evaporation of an EtOH/water mixture of zinc(II) nitrate and 4PNA (1 : 2 metal : ligand ratio) over a period of one week. The Zn(II) atom lies on an inversion centre and the structure of **3** is very similar to that of **1** except that the poorer ligating properties of the nitrate anion and smaller size of zinc(II) result in monodentate coordination and completion of the coordination sphere by two adventitious water molecules. The nitrogen atom of the amide moiety forms hydrogen bonds to the oxygen atom of the nitrate anion ($\text{N}\cdots\text{O} = 2.920(2) \text{ \AA}$, $\angle\text{N-H}\cdots\text{O} = 161(2)^\circ$) and the oxygen atoms are hydrogen-bonded to the metal-coordinated water molecules. These hydrogen bonding interactions result in the formation of a 2D hydrogen-bonded network (Fig. 6b).

Crystalline structure of $[\text{Cd}(\text{4PNA})_2(\text{NO}_3)_2(\text{H}_2\text{O})_2]$. Crystallization of 4PNA from a solution of cadmium(II) nitrate in EtOH/water at a 1 : 2 metal : ligand ratio gives a complex of formula $[\text{Cd}(\text{4PNA})_2(\text{NO}_3)_2(\text{H}_2\text{O})_2]$ (**4**) with cadmium(II) lying on an inversion centre, which is isomorphous with **3**. Although the metal–ligand bond distances are slightly longer than those in the zinc analogue, the hydrogen bonding patterns are similar (for example, the amide moiety and oxygen atom of the nitrate anion, $\text{N}\cdots\text{O} = 2.959(4) \text{ \AA}$, $\angle\text{N-H}\cdots\text{O} = 164.0^\circ$), resulting in the formation of a 2D hydrogen-bonded network (Fig. S4, ESI†).

It is quite interesting to note that in all these structures, the $\text{N-H}\cdots\text{O}$ synthon is observed where the nitrogen atom of the amide moiety of 4PNA is hydrogen-bonded to the oxygen atom of the metal-coordinated anion. Comparison of the

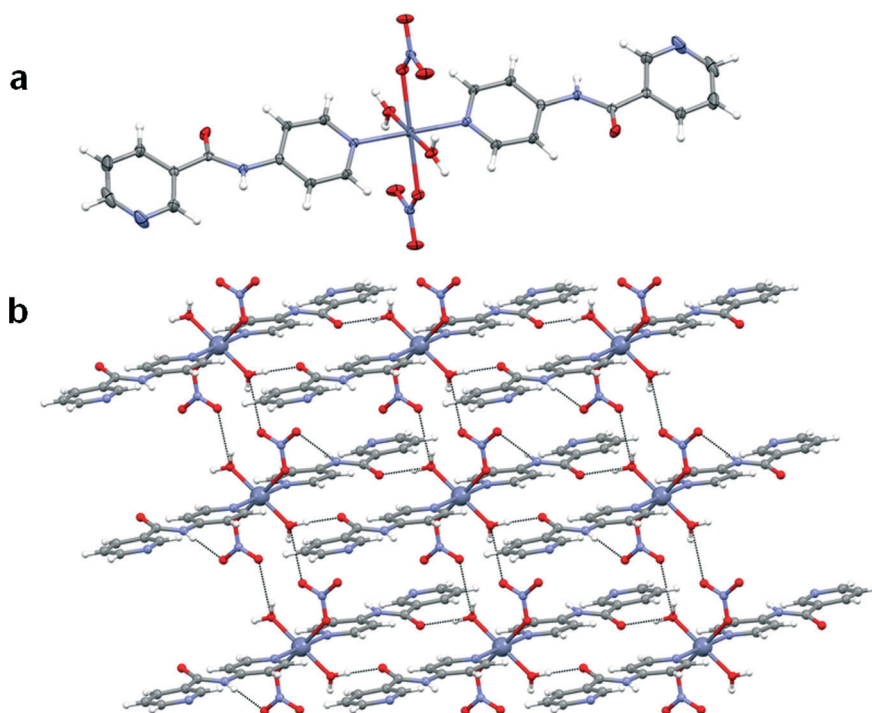


Fig. 6 (a) Molecular structure of **3** and (b) the 2D hydrogen-bonded chain observed in the solid state.



hydrogen bonding distances clearly indicates that compound 1 has strong hydrogen bonds ($N\cdots O = 2.8188(19) \text{ \AA}$). These strong interactions may be attributed to the lack of water molecules, resulting in a large electron density around the donor atom, thereby forming a rigid 1D network which could account for its gelation ability.

X-ray powder diffraction (XRPD)

It is interesting to note that the hydrogen bonding pattern in compound 1 is 1D, whereas the solid state structures of non-gelators 2, 3 and 4 are 2D hydrogen-bonded networks. In order to determine whether these single crystal structures are of relevance to the gels formed by the copper(II) complexes with a stoichiometry of 1:2, we compared the XRPD pattern calculated from the single crystal data with the experimental patterns of the xerogel obtained from DMF/water and the bulk precipitate from EtOH/water (Fig. 7). These data showed that the structure of the aqueous DMF-derived copper acetate xerogel is similar to that of the single crystal despite the fact that the sample crystallized from a different solvent. The precipitate obtained from aqueous ethanol is also the same solid form. Given the simple nature of the complex in 1, its 1:2 stoichiometry which matches the ratio needed for optimal gelation and the persistence of this solid form in all three samples, we believe that this complex is the gelator and the formation of a 1D hydrogen-bonded tape due to the lack of coordinated water is a key factor in the gelation behaviour.

While the structural information on the copper(II) chloride complex was not available due to the lack of single crystals, we have performed Cambridge Structural Database (CSD)⁵⁴ analysis and found that 91% of the copper(II) chloride structures do not have coordinated water molecules (ESI†). This might be the reason that the copper(II) chloride complex of 4PNA shows excellent gelation properties. Although the structure of the copper(II) nitrate complex of 4PNA has not been determined, the closely related *N*-phenyl-4-pyridinecarboxamine (4PPC) complex $[\text{Cu}(\text{4PPC})_2(\text{NO}_3)_2(\text{H}_2\text{O})_2]$ contains two

aqua ligands,⁵⁵ suggesting that the relatively inefficient gelation behaviour of the copper(II) nitrate complex of 4PNA may also arise from additional water hydrogen bonding interactions. The perchlorate and sulphate salts of copper(II) are known to have coordinated water molecules. The fact that these copper(II) complexes do form weak gels at high weight percent, as opposed to the crystalline complexes expected for the other hydrated metal complexes, may arise from the Jahn–Teller distorted nature of copper(II) meaning that water is relatively weakly bound in comparison to the zinc(II) analogue. Further evidence for the hydrated nature of the copper(II) complexes of 4PNA comes from the IR spectrum of the material. We compared the IR spectra of the complexes (as-synthesised) with those of the xerogels. The IR spectra of the xerogels of copper(II) acetate and the crystals were similar. The other complexes displayed a slight broad $\nu(\text{OH})$ band compared to the bulk solid (as-synthesised), which supports the effect of metal-bound water in the gelation process (Fig. S8–S12, ESI†).

Conclusions

The gelation ability of 4PNA was analysed in the presence of the salts of various metal ions such as manganese(II), iron(II), cobalt(II), nickel(II), copper(II), zinc(II) and cadmium(II). Interestingly, gelation of 4PNA metal complexes was observed only in the case of copper(II) salts. The selective gelation of all the copper(II) salts compared to the other metal salts may be attributed to the Jahn–Teller distorted nature of copper(II), which weakens water binding in all copper(II) salts. Specifically, the copper(II) acetate complex of 4PNA is a good gelator of polar solvents while the analogous zinc and cadmium nitrate and acetate complexes do not form metallogels. We suggest that this selective gelation ability of the copper(II) acetate salt has a structural origin and is correlated with the lack of coordinated water in the complex gelators, preventing 2D hydrogen-bonded network formation and favouring the formation of 1D hydrogen-bonded fibrils. An interesting feature of the gelators is the availability of non-coordinated pyridyl nitrogen atoms for further modification³⁴ and work directed towards the incorporation of metallic nanoparticles using these anchor points is currently in progress.

Acknowledgements

We are thankful to Prof. P. Dastidar, IACS-Kolkatta, India for the support and help with the initial results. We thank ÍSOR Iceland (Dr. Sigurður Sveinn Jónsson) for powder X-ray diffraction analysis and Nýsköpunarmiðstöð Íslands (Dr. Jón Matthíasson and Dr. Birgir Jóhannesson) for help in collecting the SEM images. KKD thanks the University of Iceland Start-up Grant and Research Fund (6459 and 7274) for funding.

Notes and references

- 1 S. Banerjee, R. K. Das and U. Maitra, *J. Mater. Chem.*, 2009, **19**, 6649–6687.

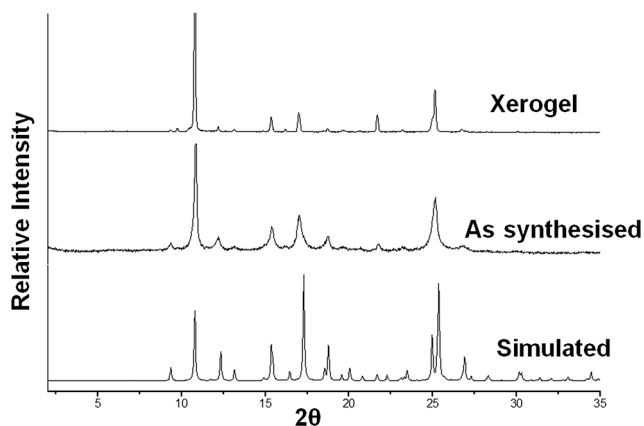


Fig. 7 XRPD data for the copper(II) acetate/4PNA xerogel and precipitated product and the simulated pattern from the single crystal X-ray data.



- 2 P. Dastidar, *Chem. Soc. Rev.*, 2008, 37, 2699–2715.
- 3 M. de Loos, B. L. Feringa and J. H. van Esch, *Eur. J. Org. Chem.*, 2005, 2005, 3615–3631.
- 4 L. A. Estroff and A. D. Hamilton, *Chem. Rev.*, 2004, 104, 1201–1218.
- 5 M. George and R. G. Weiss, *Acc. Chem. Res.*, 2006, 39, 489–497.
- 6 A. R. Hirst, B. Escuder, J. F. Miravet and D. K. Smith, *Angew. Chem., Int. Ed.*, 2008, 47, 8002–8018.
- 7 D. K. Kumar and J. W. Steed, *Chem. Soc. Rev.*, 2014, 43, 2080–2088.
- 8 M.-O. M. Piepenbrock, G. O. Lloyd, N. Clarke and J. W. Steed, *Chem. Rev.*, 2010, 110, 1960–2004.
- 9 J. W. Steed, *Chem. Soc. Rev.*, 2010, 39, 3686–3699.
- 10 G. Yu, X. Yan, C. Han and F. Huang, *Chem. Soc. Rev.*, 2013, 42, 6697–6722.
- 11 E. Krieg, H. Weissman, E. Shirman, E. Shimon and B. Rybtchinski, *Nat. Nanotechnol.*, 2011, 6, 141–146.
- 12 S. Sutton, N. L. Campbell, A. I. Cooper, M. Kirkland, W. J. Frith and D. J. Adams, *Langmuir*, 2009, 25, 10285–10291.
- 13 P. D. Thornton, R. J. Mart, S. J. Webb and R. V. Uljijn, *Soft Matter*, 2008, 4, 821–827.
- 14 K. J. C. van Bommel, M. C. A. Stuart, B. L. Feringa and J. van Esch, *Org. Biomol. Chem.*, 2005, 3, 2917–2920.
- 15 B. Li, L. Tang, L. Qiang and K. Chen, *Soft Matter*, 2011, 7, 963–969.
- 16 Q. Wei and S. L. James, *Chem. Commun.*, 2005, 1555–1556.
- 17 J. A. Foster, M.-O. M. Piepenbrock, G. O. Lloyd, N. Clarke, A. K. Howard-Judith and J. W. Steed, *Nat. Chem.*, 2010, 2, 1037–1043.
- 18 L. Meazza, J. A. Foster, K. Fucke, P. Metrangolo, G. Resnati and J. W. Steed, *Nat. Chem.*, 2013, 5, 42–47.
- 19 R. G. Weiss, P. Terech and Editors, *Molecular Gels: Materials with Self-Assembled Fibrillar Networks*, Springer, 2006.
- 20 A. Y.-Y. Tam and V. W.-W. Yam, *Chem. Soc. Rev.*, 2013, 42, 1540–1567.
- 21 N. N. Adarsh, P. Sahoo and P. Dastidar, *Cryst. Growth Des.*, 2010, 10, 4976–4986.
- 22 B. Xing, M.-F. Choi and B. Xu, *Chem. Commun.*, 2002, 362–363.
- 23 R. Gavara, J. Llorca, J. C. Lima and L. Rodriguez, *Chem. Commun.*, 2013, 49, 72–74.
- 24 T. Ishi-i, R. Iguchi, E. Snip, M. Ikeda and S. Shinkai, *Langmuir*, 2001, 17, 5825–5833.
- 25 K. Isozaki, K. Ogata, Y. Haga, D. Sasano, T. Ogawa, H. Kurata, M. Nakamura, T. Naota and H. Takaya, *Chem. Commun.*, 2012, 48, 3936–3938.
- 26 D. López and J.-M. Guenet, *Macromolecules*, 2001, 34, 1076–1081.
- 27 P. Terech, G. Gebel and R. Ramasseul, *Langmuir*, 1996, 12, 4321–4323.
- 28 Y. Zhang, B. Zhang, Y. Kuang, Y. Gao, J. Shi, X. X. Zhang and B. Xu, *J. Am. Chem. Soc.*, 2013, 135, 5008–5011.
- 29 N. N. Adarsh and P. Dastidar, *Cryst. Growth Des.*, 2011, 11, 328–336.
- 30 X. de Hatten, N. Bell, N. Yufa, G. Christmann and J. R. Nitschke, *J. Am. Chem. Soc.*, 2011, 133, 3158–3164.
- 31 T. D. Hamilton, D.-K. Bučar, J. Baltrusaitis, D. R. Flanagan, Y. Li, S. Ghorai, A. V. Tivanski and L. R. MacGillivray, *J. Am. Chem. Soc.*, 2011, 133, 3365–3371.
- 32 T. Ishiwata, Y. Furukawa, K. Sugikawa, K. Kokado and K. Sada, *J. Am. Chem. Soc.*, 2013, 135, 5427–5432.
- 33 M. Paul, N. N. Adarsh and P. Dastidar, *Cryst. Growth Des.*, 2012, 12, 4135–4143.
- 34 M.-O. M. Piepenbrock, N. Clarke and J. W. Steed, *Soft Matter*, 2011, 7, 2412–2418.
- 35 K. Hanabusa, Y. Maesaka, M. Suzuki, M. Kimura and H. Shirai, *Chem. Lett.*, 2000, 1168–1169.
- 36 S. Bhattacharjee and S. Bhattacharya, *Chem. Commun.*, 2014, 50, 11690–11693.
- 37 S. Bhattacharjee, S. K. Samanta, P. Moitra, K. Pramoda, R. Kumar, S. Bhattacharya and C. N. R. Rao, *Chem. – Eur. J.*, 2015, 21, 5467–5476.
- 38 P. Kumar Vemula, U. Aslam, V. Ajay Mallia and G. John, *Chem. Mater.*, 2007, 19, 138–140.
- 39 M. Paul, K. Sarkar and P. Dastidar, *Chem. – Eur. J.*, 2015, 21, 255–268.
- 40 G. R. Desiraju, *Angew. Chem., Int. Ed. Engl.*, 1995, 34, 2311–2327.
- 41 T. Klawonn, A. Gansauer, I. Winkler, T. Lauterbach, D. Franke, R. J. M. Nolte, M. C. Feiters, H. Borner, J. Hentschel and K. H. Dotz, *Chem. Commun.*, 2007, 1894–1895.
- 42 P. Sahoo, V. G. Puranik, A. K. Patra, P. U. Sastry and P. Dastidar, *Soft Matter*, 2011, 7, 3634–3641.
- 43 A. Y.-Y. Tam, K. M.-C. Wong and V. W.-W. Yam, *J. Am. Chem. Soc.*, 2009, 131, 6253–6260.
- 44 B. Xing, M.-F. Choi and B. Xu, *Chem. – Eur. J.*, 2002, 8, 5028–5032.
- 45 S. Yoon, W. J. Kwon, L. Piao and S.-H. Kim, *Langmuir*, 2007, 23, 8295–8298.
- 46 P. Byrne, G. O. Lloyd, L. Applegarth, K. M. Anderson, N. Clarke and J. W. Steed, *New J. Chem.*, 2010, 34, 2261–2274.
- 47 D. K. Kumar, D. A. Jose, P. Dastidar and A. Das, *Langmuir*, 2004, 20, 10413–10418.
- 48 O. V. Dolomanov, L. J. Bourhis, R. J. Gildea, J. A. K. Howard and H. Puschmann, *J. Appl. Crystallogr.*, 2009, 42, 339–341.
- 49 G. Sheldrick, *Acta Crystallogr., Sect. A: Found. Crystallogr.*, 2008, 64, 112–122.
- 50 J. H. Lee, S. Kang, J. Y. Lee and J. H. Jung, *Soft Matter*, 2012, 8, 6557–6563.
- 51 Z. Džolić, M. Cametti, D. Milić and M. Žinić, *Chem. – Eur. J.*, 2013, 19, 5411–5416.
- 52 S. Sarkar, S. Dutta, S. Chakrabarti, P. Bairi and T. Pal, *ACS Appl. Mater. Interfaces*, 2014, 6, 6308–6316.
- 53 T. K. Adalder, U. K. Das, J. Majumder, R. Roy and P. Dastidar, *J. Indian Inst. Sci.*, 2014, 94, 9–24.
- 54 F. Allen, *Acta Crystallogr., Sect. B: Struct. Sci.*, 2002, 58, 380–388.
- 55 G. Chun-Hua, Z. Xiang-Dong, G. Wei, G. Fang and L. Qi-Tao, *Chin. J. Chem.*, 2005, 23, 1001–1006.

